HHS Public Access

Author manuscript

Biopolymers. Author manuscript; available in PMC 2015 July 13.

Published in final edited form as:

Biopolymers. 2010 May ; 93(5): 442–450. doi:10.1002/bip.21356.

VCD Spectroscopic Properties of the β-hairpin Forming Miniprotein CLN025 in Various Solvents

Marcus P. D. Hatfield, **Richard. F. Murphy**, and **Sándor Lovas***

Department of Biomedical Sciences, Creighton University, Omaha, NE 68178, U.S.A.

Abstract

Electronic and vibrational circular dichroism are often used to determine the secondary structure of proteins, because each secondary structure has a unique spectrum. In order to determine these spectral features, polypeptides that are known to adopt a particular conformation along their entire length are studied ideally. Little is known about the vibrational circular dichroic spectroscopic features of the β-hairpin. In this study, the VCD spectral features of a decapeptide, YYDPETGTWY (CLN025), which forms a stable β-hairpin that is stabilized by intramolecular weakly polar interactions and hydrogen bonds were determined. Molecular Dynamics simulations and ECD spectropolarimetry were used to confirm that CLN025 adopts a β-hairpin in water, TFE, MeOH and DMSO and to examine differences in the secondary structure, hydrogen bonds and weakly polar interactions. CLN025 was synthesized by microwave-assisted solid phase peptide synthesis with N^{α}-Fmoc protected amino acids. The VCD spectra displayed a (−,+,−) pattern with bands at 1640 to 1656 cm^{-1}, 1667 to 1687 cm^{-1} and 1679 to 1686 cm^{-1} formed by the overlap of a lower frequency negative couplet and a higher frequency positive couplet. A maximum IR absorbance was observed at 1647 to 1663 cm^{-1} with component bands at 1630 cm^{-1}, 1646 cm^{-1}, 1658 cm^{-1} and 1675 to 1680 cm^{-1} that are indicative of the β-sheet, random meander, either random meander or loop and turn, respectively. These results are similar to the results of others, who examined the VCD spectra of β-hairpins formed by ^{D}Pro-Xxx turns and indicate that observed pattern is typical of β-hairpins.

Keywords

CLN025; Chignolin; vibrational circular dichroism; electronic circular dichroism; beta-hairpins; miniprotein; molecular dynamics

Introduction

Model β-hairpin miniproteins are frequently studied because they are the simplest form of anti-parallel β-sheet and often display characteristics indicative of proteins such as two-state folding.[1] β-hairpins are stabilized by cross-strand hydrogen bonds, disulfide bonds and weakly polar interactions.[2–4] Weakly polar interactions play an important role due to their strength and ubiquitousness in peptides. Weakly polar interactions can be as strong as

*Corresponding author. Address: Department of Biomedical Sciences, Criss II, Room 313, Creighton University, 2500 California Plaza, Omaha, NE 68178, Phone: 402-280-5753, Fax: 402-280-2690, slovas@creighton.edu.

hydrogen bonds.[5–12] They play an important role in the stabilization of secondary structure such as α-helices,[5] and the tertiary structure of peptides such as the TC5b[8] and APP[10, 12] miniproteins. Numerous β-hairpins have been designed to take advantage the aromatic-aromatic (Ar-Ar) interactions,[13–17] cation-π interactions,[16–18] and CH-π interactions.[16, 17]

CLN025, Tyr-Tyr-Asp-Pro-Glu-Thr-Gly-Thr-Trp-Tyr, (Figure 1), is a miniprotein that forms a stable β-hairpin with a T_m of 70 °C, which undergoes a reversible cooperative transition upon thermal denaturation.[19] CLN025 is a chignolin variant in which the terminal Gly residues are replaced with Tyr residues. The β-hairpin has a turn-initiating Asp-Pro sequence,[20] and is stabilized by an Ar-Ar interaction between the side chains of Tyr2 and Trp9 and hydrogen bonds between Asp3 and Thr6, Gly7 and Thr8.[19]

The vibrational circular dichroism spectroscopic properties of helices,[21–24] turns,[6, 25–27] random meander[23, 28] and β-sheets[23, 27, 29–31] have been studied extensively but the properties of the β-hairpin have not. Previous studies of the VCD spectroscopic properties of β-hairpins were of peptides with ^{D}Pro-Xxx turns or head-to-tail cyclization to stabilize the structure in chloroform or aqueous solvents rather than solvents such as TFE, MeOH or DMSO.[32–34] Many of the designed β-hairpins aggregate at higher concentrations in water. This hampers experiments to examine VCD spectra of β-hairpins containing only L-amino acids. In this study, the VCD spectroscopic properties of CLN025, which has been shown to form a stable β-hairpin containing only naturally occurring amino acids, in aqueous solution and in different organic solvents (TFE, MeOH and DMSO) were determined. Molecular Dynamics simulations and ECD were used to confirm the β-hairpin conformation of CLN025 in the solvents.

Methods

CLN025 synthesis and purification

CLN025 was synthesized with a CEM Liberty microwave peptide synthesizer (CEM, Matthews, NC, USA) at a 0.1 mmole scale using a H-Tyr(OtBu) HMPB ChemMatrix resin and 5 molar excess of N^{α}-Fmoc protected amino acids. t-butyl protection was used to protect the reactive side chains of Asp, Glu, Thr and Tyr while t-Boc protection was used for Trp residues. Couplings were performed using HATU and DIEA at 75 °C for 10 minutes with 25 W radiation energy. Deprotections were performed using 20% (v/v) piperidine and 0.1 M HOBt at 75 °C for 3 minutes with 35 W radiation energy.

The peptide was cleaved from the resin by stirring in a 95/2.5/2.5 (v/v/v) TFA/TIS/water mixture for 10 minutes at 0 °C followed by 110 minutes at room temperature. The peptide was precipitated with cold diethyl ether, filtered, dissolved in TFA and filtered. The filtrate was evaporated to 1 mL and the peptide was precipitated with cold diethyl ether and collected by filtration. The peptide was dissolved in glacial acetic acid which was diluted to 5% acetic acid with nanopure water and the solution was lyophilized.

Purification was performed by reverse-phase high pressure liquid chromatography using a Gilson dual pump apparatus (Gilson, Inc, Middleton, WI, USA). The peptide was purified on a Phenomenex Jupiter C18 column (5 μm, 200 mm × 10 mm; Phenomenex, Torrance,

CA, USA) using an aqueous solvent of 0.1% TFA in water and an organic solvent of 0.09% TFA in acetonitrile. The peptide was purified at 30 °C using a gradient of 10% to 50% organic solvent over 60 minutes with a flow rate of 4 mL min^{-1}. Pure fractions were pooled and lyophilized. The peptide was identified using a API150EX mass spectrometer (PE SCIEX, Foster City, CA, USA)and characterized by RP-HPLC with a Jupiter C18 column (5 μm, 200 mm × 4.6 mm; Phenomenex, Torrance, CA, USA) using a 3% to 60% organic solvent gradient over 40 minutes at 1 mL min^{-1}.

ECD

ECD spectra were recorded using a Jasco J-810 Spectropolarimeter (JASCO, Inc., Easton, MD, USA) by performing 20 scans from 185 to 250 nm at 100 nm min^{-1} scan speed in a 0.05 cm path length quartz cell. The background spectra of the solvents were subtracted and the mean residue molar ellipticities were calculated using peptide concentrations determined by quantitative RP-HPLC[35] with a Jupiter C18 column (5 μm, 200 mm × 4.6 mm; Phenomenex, Torrance, CA, USA). CLN025 was dissolved in either 20 mM KH_2PO_4-K_2HPO_4 buffer (pH 7.0), TFE or MeOH at a final concentration of 100 μM. CDSSTR[36–38] analysis was performed with data set 6 using the DichroWeb website.[39–43] The concentration of 100 μM CLN025 was used because at concentrations above 1 mM CLN025 aggregates.

VCD

CLN025 was dissolved in 0.1 M DCl in D_2O and lyophilized three times prior to VCD measurements in order to remove all trifluoroacetic acid salts and perform a H/D exchange on the backbone of the peptide. All samples for VCD measurement were prepared to have a concentration of 20 mg mL^{-1} CLN025. Buffer solutions were prepared by dissolving 4 mg of CLN025 in 10 μL DMSO-d_6 and gradually diluting this solution to 5% DMSO-d_6 with 20 mM KD_2PO_4-K_2DPO_4 buffer (pD 7.4). All other solutions were prepared by dissolving 2 mg CLN025 in either TFE-d, MeOH-d_4 or DMSO-d_6.

VCD spectra were recorded using a dual PEM BOMEM Biotools Chiralir Fourier Transform VCD Spectropolarimeter (BioTools, Inc., Jupiter, FL, USA). Either 4 or 8 block measurements consisting of 4500 scans for VCD and 225 scans for IR absorption at 8 cm^{-1} resolution were performed in a 75 μm pathlength CaF_2 cell. 8 blocks were recorded for VCD measurements of CLN025 in buffer, TFE-d, MeOH-d_4 and DMSO-d_6 at 20 °C, while 4 blocks were recorded for VCD measurements in buffer at 0 °C, 20 °C and 60 °C. Spectra of the blocks were averaged and the background spectra of the solvent and water vapor were subtracted. Spectra were set to 0 at 1800 cm^{-1} and normalized[44] by dividing each data point by the maximum IR absorbance in the amide I' region. The spectra were normalized in order to remove the effect of small differences in the sample concentration on the intensity of the spectra.

Maximum-entropy deconvolution and peak fitting analysis of the FT-IR spectra were performed with the PROTA v 3.0 software package (BioTools, Inc., Jupiter, FL, USA) using the tyrosyl C-C ring vibration band at 1515 cm^{-1} as the representative peak shape, which has been found to be a good marker due to its sharpness, narrow width, and discrete

location.[45] Peak-fitting analysis is not conclusive, because it produces no unique band assignment, molar absorptivities of all conformations are assumed to be equal and conclusions can be subjective.[46] The analysis performed by the PROTA software package, however is less subjective, by using Bayesian derivatives and maximum likelihood functions to generate a list of peaks that meet acceptable signal to noise criteria and determines the areas of the individual peaks with the Levenberg-Marquardt maximum likelihood algorithm.

Molecular Dynamics Simulations

Molecular Dynamics simulations were performed using the crystal structure of CLN025[19] with the GROMACS 3.2.1 software package[47, 48] using the GROMOS 96 force field with the 53a6 parameter set.[49, 50] CLN025 was solvated in either 1438 SPC[51] water, 302 TFE, 1866 MeOH or 286 DMSO molecules in a 45.61 nm^3 dodecahedral box with one chloride and three sodium ions to neutralize the system. The MeOH, TFE and DMSO models used were optimized for the 53a6 parameter set[52] and the experimentally determined compressibilities (4.92×10^{-5} bar^{-1}, 4.50×10^{-5} bar^{-1}, 4.45×10^{-5} bar^{-1}, 1.22×10^{-4} bar^{-1}, 1.29×10^{-4} bar^{-1}, 4.50×10^{-5} bar^{-1}) and dielectric constants (86, 78, 68, 27, 32, 47) were used for the simulations of CLN025 in SPC water at 278 K, 300 K and 333 K and TFE, MeOH and DMSO at 300 K, respectively.[53] The solvated structures were energy-minimized using steepest descent.[54] An NVT simulation of the positionally restrained peptide was performed for 100 ps at 300 K (27 °C) followed by a 200.1 ns NPT simulation at 300 K and 1 bar using Berendsen coupling.[55] All bonds were constrained[56] with Shake[57] in the TFE simulation and Lincs[58] in the other simulations. In addition, MD simulations were performed in SPC water at 278 K (5 °C) and 333 K (60 °C).

MD simulations were analyzed by examining the middle structure of the largest cluster determined by the backbone RMSD of structures sampled every 10 ps along the trajectory. Secondary structure of CLN025 was analyzed by the DSSP method.[59]

Results and Discussion

ECD spectroscopy

The ECD spectra of 100 μM CLN025 in 20 mM potassium phosphate buffer (pH 7.0) from 0 °C to 80 °C and cooled from 80 °C to 0 °C are shown in Figure 2. These spectra are similar to those measured by Honda and coworkers,[19] except their spectra showed a more intense negative band at 197 nm. The spectra indicate that the peptide has β-sheet, type II β-turn and random meander, as well as an aromatic couplet caused by the Ar-Ar interactions.

As the temperature increases, the intensity and position of the positive band of the aromatic couplet shifts from 225 to 230 nm and at some temperatures more than one couplet is apparent most likely due to contributions from the Tyr2-Trp9 and Tyr1-Tyr10 Ar-Ar interactions as well as the Tyr1-Tyr9 interaction at higher temperatures. This provides further evidence that using the aromatic couplet as a measure of folding is not accurate since, in peptides containing more than two aromatic rings, the interactions could shift causing a shift in the aromatic couplet that is not indicative of the overall fold.

As the temperature increases above 60 °C a positive band at 212 nm becomes visible. This is indicative of random meander, indicating that the β-hairpin is destabilized. The increase in random meander content most likely results from a loss of β-sheet which would explain why the intensity of the 195 nm band does not change. The spectra, however, still suggests β-hairpin conformation and the aromatic couplet indicates that the ends of the peptide remain in close proximity. The ECD spectra of the peptide at 0 °C and the peptide cooled from 80 °C to 0 °C are similar, indicating reversible unfolding.

The ECD spectra of CLN025 in buffer, TFE and MeOH are shown in Figure 3. The spectra have similar characteristics, but the peaks in the spectrum in TFE are blue-shifted 2 to 3 nm while in MeOH they are red shifted 1 to 2 nm from the positions in the spectrum of the peptide in buffer. This is most likely due to solvent effects including differing degrees of hydration of individual amide groups[46, 60–62] and differences in the dipolar character of the solvent.[63–66] The aromatic couplet in TFE is less intense due to the tendency of high concentrations of TFE to weaken the interactions between hydrophobic side chains.[67, 68] The higher intensity of the aromatic couplet in MeOH suggests a stronger Ar-Ar interaction. Due to the overlap of the aromatic couplet with signals conveying information about the secondary structure,[69, 70] it is difficult to determine if small changes in the conformation of the peptide occur in the different solvents. CDSSTR analysis (Table 1) however, suggests that the peptide is 46% sheet, 23% turn and 31% random meander in buffer. In TFE and MeOH, the sheet component increases to 56% and 59%, respectively, while the random meander component decreases to 20% in TFE and the turn component decreases to 13% in MeOH.

The ECD spectra of CLN025 are similar at all temperatures and in the different solvents indicating no significant conformational change in the structure of CLN025 upon heating and in either TFE or MeOH. This demonstrates the stability of the β-hairpin in CLN025. The small changes in the ECD spectra of CLN025 indicate that at high temperatures the amount of random meander increases and the Ar-Ar interactions decrease. In TFE, CLN025 displays a higher β-sheet content and a decrease in the amount of random meander. In MeOH, the β-sheet and random meander content of CLN025 increase and the turn content decreases.

VCD spectroscopy

The VCD and FT-IR spectra of CLN025 in various solvents are shown in Figure 4 and the position of the VCD bands are listed in Table 2. The IR spectrum of CLN025 in buffer has a maximum absorbance at 1647 cm^{-1} with shoulders at 1675 cm^{-1}, 1646 cm^{-1}, 1630 cm^{-1} and 1612 cm^{-1} in the deconvoluted spectra, which are indicative of turn, random meander, β-sheet and tertiary amide or tyrosine side-chain vibration, respectively.[15, 23, 27, 45, 71] The VCD spectra show a (−,+,−) pattern, formed by the overlap of the positive bands of a negative and positive couplet, with bands at 1640 cm^{-1}, 1667 cm^{-1} and 1679 cm^{-1}, respectively. The first couplet, centered at 1653 cm^{-1}, is indicative of random meander and may indicate a local left handed twist[28] while the second couplet, centered at 1673 cm^{-1}, is indicative of a type II' β-turn.[25, 72]

The IR absorbance spectra of the peptide in TFE and MeOH are similar to the IR spectrum of the peptide in buffer, except the maximum absorbance is shifted to 1655 cm^{-1}. The peaks

of the VCD spectra of the peptide in TFE and MeOH are also shifted from positions in buffer with the negative band shifted to 1647 cm^{-1} and the positive band to 1671 cm^{-1}. In MeOH the second negative VCD band is at the same location as the second negative VCD band of the peptide in buffer, while in TFE this band is shifted up to 1686 cm^{-1} which indicates a change in the turn structure of CLN025 in TFE.

In DMSO, the maximum IR absorbance is shifted to 1663 cm^{-1} and the 1612 cm^{-1} absorbance peak is resolved due to a reduced shoulder around 1630 cm^{-1}, indicating a loss of β-sheet. The peaks at 1706 cm^{-1} and 1712 cm^{-1} are indicative of the Glu and Asp side chains in deuterated solvents, respectively,[45] or a change in the turn-like structure of the peptide. The VCD of CLN025 in DMSO shows only a negative couplet with a negative component at 1656 cm^{-1} and positive component at 1687 cm^{-1}, attributed to a greater relaxation of the turn that causes the second couplet to be obscured by the first couplet.

Peak-fitting analysis of the FT-IR spectra, shown in Table 3, indicates that the 1612 cm^{-1} signal contributes equally in the different solvents, which indicates that the environment around the prolyl residue does not change significantly. The 1630 cm^{-1} signal indicates that CLN025 is approximately 16%, 24% and 11% β-sheet in buffer, TFE and MeOH, respectively, while a signal accounting for 3% of the amide I' area in DMSO is due either to β-sheet or the low frequency absorbance of turn structures. The signals at 1646 cm^{-1} and 1658 cm^{-1} are due either to random meander of loop conformations. The major signal shifts from 1646 cm^{-1} to 1658 cm^{-1} when the peptide is in non-aqueous solutions, which causes the shift of the negative VCD couplet in these solvents. The signal at 1675 cm^{-1} is due either to the turn or the high frequency absorbance of β-sheet[23, 45] although turn is more likely due to the high signal of this peak in DMSO. The shift of the 1675 cm^{-1} band to 1680 cm^{-1} in TFE is the likely cause of the shift in the positive couplet in the VCD spectrum. The 1705 cm^{-1} peak in TFE and MeOH is most likely to be due to the glutamic acid side chain, indicating that this side chain is not shielded. The 1712 cm^{-1} band seen in buffer and especially in DMSO, where it accounts for 25% of the amide I' signal, is due either to the aspartic acid side chain or a change in structure. The aspartic acid side chain provides a better explanation due to the lack of a VCD signal in this region and because of the shift in the orientation of the side chain in the structure of CLN025 in DMSO (Figure 6d).

The CDSSTR analysis of the ECD spectra (Table 1) and the peak fitting analysis of the FT-IR spectra (Table 3) show similarities in the differences of β-sheet, turn and random meander content in different solvents. Each analysis indicates that in TFE the β-sheet content of CLN025 increases and the random meander content decreases. In MeOH, both analyses indicate a loss of turn content but the peak-fitting analysis indicates a slight loss of β-sheet and an increase in the random meander content of CLN025. This discrepancy between the results of the two analyses is most probably due to the interference of the signal from the aromatic couplet in the ECD spectra. Even though the amount of turn in the peptide in MeOH decreases, the position of the second couplet and the relative contributions of the amide bands at 1646 cm^{-1} and 1658 cm^{-1} suggest that the turn in the peptide in MeOH is more similar to that in buffer than the turn in TFE is to that in buffer. While the CDSSTR analysis of the ECD spectra of CLN025 in buffer indicates that the β-hairpin is 46% sheet, 23% turn and 31% random meander, the peak fitting analysis of the VCD indicates that the

β-hairpin is 16% sheet, 12% turn and 67% random meander. The major differences between the overall amounts of the β-sheet, turn and random meander assigned by the two analyses could be due to the interference of the aromatic couplet in the ECD spectra and the faulty assumption in peak fitting analysis that the molar absorbtivities of all conformations are equal.[46]

The VCD spectra of CLN025 in buffer at 5 °C, 20 °C and 60 °C, shown in Figure 5, are similar indicating that the β-hairpin is stable. The less pronounced shoulder at 1630 cm^{-1} in the IR absorption spectrum indicates that the amount of β-sheet content decreases at 60 °C.

The analysis indicates that the VCD spectra of CLN025 and β-hairpins in general consist of overlapping negative and positive couplets. The negative couplet is due to random meander or loop structure, while the higher frequency positive couplet is due to the turn. This produces a (−,+,−) pattern with bands at 1640 to 1656 cm^{-1}, 1667 to 1687 cm^{-1} and 1679 to 1686 cm^{-1}. The β-sheet component of the VCD spectra is not visible due to its low intensity[29] and overlap with the first negative band (1640 to 1656 cm^{-1}). The β-sheet, however, might contribute to the greater width of the first negative band. The IR absorption spectra show a broad amide I' band with a maximum at 1647 to 1663 cm^{-1} and bands at 1630 cm^{-1}, 1646 cm^{-1}, 1658 cm^{-1} and 1675 to 1680 cm^{-1} which are indicative of the β-sheet, random meander, random meander or loop and turn, respectively. The shifts in the peaks of the VCD and IR absorption spectra of the peptides in the different solvents is likely to be due to solvent effects, which have been shown to alter the spectral shapes of β-hairpins due to differing degrees of hydration of the individual amide groups[46, 60–62] and differences in the dipolar character of the solvent.[63–66]

The results are similar to the results found by other groups for β-hairpins that have ^{D}Pro-Xxx turns. Zhao and coworkers[32] examined the spectra of numerous octapeptides with a ^{D}Pro-Xxx turn in chloroform and found a (−,+,−,+) pattern of VCD peaks at 1643 to 1659 cm^{-1}, 1655 to 1670 cm^{-1}, 1670 to 1678 cm^{-1} and 1690 to 1697 cm^{-1}, respectively with a maximum IR absorbance at 1690 to 1697 cm^{-1}. Hilario and associates[33] examined the VCD spectra of a dodecapeptide with a ^{D}Pro-Gly turn in aqueous solution and found a negative couplet with negative band at 1638 cm^{-1}, positive band at 1660 to 1680 cm^{-1} in the VCD spectra and a maximum IR absorbance at 1638 cm^{-1}. These results are similar to those here, except that the maximum IR absorbance was 9 cm^{-1} lower. This is most likely to be due to a greater amount of β-sheet structure in dodecapeptide. Hilario and coworkers[34] examined spectra of 4 to 16 residue peptides with a ^{D}Pro-Gly turn in aqueous solution and found a negative couplet with negative band at 1635 to 1645 cm^{-1} and positive band at 1660 to 1670 cm^{-1} in the VCD spectra and a maximum IR absorbance at 1635 to 1645 cm^{-1}.

MD simulations

Cluster analysis, based on the backbone RMSD of the peptide, generated 8, 15, 76, 3, 19 and 6 clusters for CLN025 in H_2O at 5 °C, H_2O at 27 °C, H_2O at 60 °C, TFE at 27 °C, MeOH at 27 °C and DMSO at 27 °C, respectively. The middle structures of the largest clusters are seen in Figure 9 and account for 92.3%, 94.4%, 72%, 99.8%, 83.9% and 98.2%, respectively, of the 20,000 structures sampled. The small number of clusters and the large contribution of the largest cluster indicates the CLN025 forms a stable structure in all

environments studied. The middle structures indicate that the β-hairpin conformation is maintained in all environments but the turn is relaxed in TFE and DMSO showing a random meander from Pro4 to Gly7 in TFE and from Asp3 to Gly7 in DMSO. In DMSO the Asp3 side chain moves closer to the opposite strand and rotates so that the oxygen atoms are pointing towards the turn and strand. This allows the side chain to participate in more hydrogen bonds. In MeOH, the peptide maintains a tight turn though shortened and the Gly7 residue is assigned to the β-sheet region. In H_2O at 60 °C, the turn is flattened causing the Gly7 residue to rotate and the C-terminal strand changes conformation by elongation. This causes the hydrogen bond pattern to change and the Trp9 residue to move further away from the Tyr2 residue breaking the Ar-Ar interaction and forming a new Ar-Ar interaction with the Tyr1 residue.

DSSP analysis (Figure 7) further confirms that the β-hairpin structure of CLN025 in all environments studied has a Pro-Glu-Thr-Gly turn flanked by two residues on each side in a β-sheet or β-bridge conformation. At 60 °C, Trp9 changes from being in a β-sheet conformation to a random meander conformation. In DMSO, the β-sheet structure of the peptide is diminished significantly. Tyr2 and Trp9 form a β-bridge, the turn is relaxed and the Asp3, Gly7 and Thr8 residues are in a random meander conformation.

The MD simulations confirm the results of the ECD and VCD spectral analyses. CLN025 maintained a β-hairpin conformation in all environments studied. In TFE, the turn is relaxed as shown by the shift in the second couplet of the VCD spectra and its corresponding amide I' bands in the IR spectra as well as by the middle structures of the most populated cluster from the MD simulations and the DSSP analysis. In MeOH, the turn in CLN025 is shortened, as seen by the loss of turn content from the CDSSTR analysis of the ECD spectra, the results of the peak-fitting analysis of the VCD spectra and the middle structure of the peptide in MD analyses. In MeOH, however, the peptide maintains the same tight conformation as the peptide in water as indicated by the position of the second couplet in the VCD spectra and the assignment of the turn region in the middle structures of the peptide. In DMSO, the turn is relaxed and is mostly random meander as seen by the lack of an evident second couplet in the VCD spectra as well as by the DSSP analysis and the middle MD structures of the peptide.

Conclusions

The VCD spectral properties of a 10 residue miniprotein, CLN025, that forms a stable β-hairpin, with only naturally occurring amino acids and without D-amino acids or cyclization to stabilize the β-hairpin, are reported. ECD, VCD and Molecular Dynamics simulations confirm that CLN025 adopts a stable β-hairpin conformation in the environments studied. The VCD spectra exhibit a (−,+,−) pattern with bands at 1640 to 1656 cm^{-1}, 1667 to 1687 cm^{-1} and 1679 to 1686 cm^{-1}. A maximum IR absorbance was observed at 1647 to 1663 cm^{-1} with bands at 1630 cm^{-1}, 1646 cm^{-1}, 1658 cm^{-1} and 1675 to 1680 cm^{-1} in the deconvoluted spectra, indicating β-sheet, random meander, random meander or loop and turn, respectively. These results are similar to those reported for peptides in which ^{D}Pro was incorporated to nucleate the β-turn in the hairpin and suggest that the VCD and IR absorbance spectra reported here are typical of β-hairpins.

Acknowledgments

This work was supported by the NIH-INBRE grant P20 RR016469.

References

1. Ptitsyn OB. FEBS Lett. 1991; 131:197.
2. Ramirez-Alvarado M, Kortemme T, Blanco FJ, Serrano L. Bioorg & Med Chem. 1999; 7:93–103. [PubMed: 10199660]
3. Maynard AJ, Sharman GJ, Searle MS. J Am Chem Soc. 1998; 120:1996–2007.
4. Andersen NH, Dyer RB, Fesinmeyer RM, Gai F, Liu Z, Neidigh JW, Tong H. J Am Chem Soc. 1999; 121:9879–9880.
5. Palermo NY, Csontos J, Owen MC, Murphy RF, Lovas S. J Comput Chem. 2007; 28:1208–1214. [PubMed: 17299770]
6. Borics A, Murphy RF, Lovas S. Protein Pept Lett. 2007; 14:353–359. [PubMed: 17504093]
7. Csontos J, Palermo NY, Murphy RF, Lovas S. J Comput Chem. 2008; 29:1344–1352. [PubMed: 18172837]
8. Hatfield MPD, Palermo NY, Csontos J, Murphy RF, Lovas S. J Phys Chem B. 2008; 112:3503–3508. [PubMed: 18303883]
9. Csontos J, Murphy RF, Lovas S. Biopolymers. 2008; 89:1002–1011. [PubMed: 18615659]
10. Palermo NY, Csontos J, Murphy RF, Lovas S. Int J Quantum Chem. 2008; 108:814–819. [PubMed: 18985166]
11. Csontos J, Murphy RF, Lovas S. Adv Exp Med Biol. 2009; 611:79–80. [PubMed: 19400102]
12. Palermo NY, Csontos J, Murphy RF, Lovas S. Adv Exp Med Biol. 2009; 611:89–90. [PubMed: 19400107]
13. Cochran AG, Skelton NJ, Starovasnik MA. Proc Natl Acad Sci USA. 2001; 98:5578–5583. [PubMed: 11331745]
14. Xu Y, Oyola R, Gai F. J Am Chem Soc. 2003; 125:15388–15394. [PubMed: 14664583]
15. Takekiyo T, Wu L, Yoshimura Y, Shimizu A, Keiderling TA. Biochemistry. 2009; 48:1543–1552. [PubMed: 19173596]
16. Eidenschink LA, Kier BL, Huggins KNL, Andersen NH. Proteins. 2009; 75:308–322. [PubMed: 18831035]
17. Andersen NA, Olsen KA, Fesinmeyer Rm, Tan X, Hudson FM, Eidenschink LA, Farazi SR. J Am Chem Soc. 2006; 128:6101–6110. [PubMed: 16669679]
18. Riemen AJ, Waters ML. Biochemistry. 2009; 48:1525–1531. [PubMed: 19191524]
19. Honda S, Akiba T, Kato YS, Sawada Y, Sekijima M, Ishimura M, Ooishi A, Watanabe H, Odahara T, Harata K. J Am Chem Soc. 2008; 130:15327–15331. [PubMed: 18950166]
20. Terada T, Satoh D, Mikawa T, Ito Y, Shimizu K. Proteins. 2008; 73:621–631. [PubMed: 18473359]
21. Borics A, Murphy RF, Lovas S. Biopolymers. 2003; 72:21–24. [PubMed: 12400088]
22. Copps J, Murphy RF, Lovas S. Peptide Science. 2007; 88:427–437. [PubMed: 17326200]
23. Krimm S, Bandekar J. Adv Protein Chem. 1986; 38:181–364. [PubMed: 3541539]
24. Prestrelski SJ, Byler DM, Thompson MP. Int J Pept Protein Res. 1991; 37:508–512. [PubMed: 1917308]
25. Borics A, Murphy RF, Lovas S. Biopolymers. 2006; 85:1–11. [PubMed: 16948119]
26. Wyssbrod HR, Diem M. Biopolymers. 1992; 32:1237–1242. [PubMed: 1420990]
27. Shanmugam G, Polavarapu PL. Biophysical Journal. 2004; 87:622–630. [PubMed: 15240495]
28. Keiderling TA, Silva RAGD, Yoder G, Dukor RK. Bioorganic & Medicinal Chemistry. 1999; 7:133–141. [PubMed: 10199663]
29. Kubelka J, Keiderling TA. J Am Chem Soc. 2001; 123:12048–12058. [PubMed: 11724613]
30. Pancoska P, Yasui SC, Keiderling TA. Biochemistry. 1989; 28:5917. [PubMed: 2775742]

31. Baumruk V, Keiderling TA. J Am Chem Soc. 1993; 115:6939.
32. Zhao C, Polavarapu PL, Das C, Balaram P. J Am Chem Soc. 2000; 122:8228–8231.
33. Hilario J, Kubelka J, Syud FA, Gellman SH, Keiderling TA. Biopolymers. 2002; 67:233–236. [PubMed: 12012436]
34. Hilario J, Kubelka J, Keiderling TA. J Am Chem Soc. 2003; 125:7562–7574. [PubMed: 12812496]
35. Szendrei GI, Fabian H, Mantsch HH, Lovas S, Nyeki O, Schon I, Otvos L Jr. Eur J Biochem. 1994; 226:917–924. [PubMed: 7813483]
36. Compton LA, Johnson WC Jr. Anal Biochem. 1986; 155:155–167. [PubMed: 3717552]
37. Manavalan P, Johnson WC Jr. Anal Biochem. 1987; 167:76–85. [PubMed: 3434802]
38. Sreerama N, Woody RW. Anal Biochem. 2000; 287:252–260. [PubMed: 11112271]
39. Whitmore L, Wallace BA. Biopolymers. 2008; 89:392–400. [PubMed: 17896349]
40. Whitmore L, Wallace BA. Nucleic Acids Research. 2004; 32:W668–W673. [PubMed: 15215473]
41. Lobley A, Whitmore L, Wallace BA. Bioinformatics. 2002; 18:211–212. [PubMed: 11836237]
42. Sreerama N, Woody RW. Anal Biochem. 2000; 287:252–260. [PubMed: 11112271]
43. Sreerama N, Venyaminov SY, Woody RW. Anal Biochem. 2000; 287:243–251. [PubMed: 11112270]
44. Baumruk V, Huo D, Dukor RK, Keiderling TA, Lelieure D, Brack A. Biopolymers. 1994; 34:1115–1121. [PubMed: 8075391]
45. Jung C. J Mol Recognit. 2000; 13:325–351. [PubMed: 11114067]
46. Surewicz WK, Mantsch HH, Chapman D. Biochemistry. 1993; 32:389–394. [PubMed: 8422346]
47. Lindahl E, Hess B, Van der Spoel D. J Mol Mod. 2001; 7:306–317.
48. Berendsen HJC, Van der Spoel D, Van Drunen R. Comp Phys Comm. 1995; 91:43–56.
49. Oostenbrink C, Villa A, Mark AE, van Gunsteren WF. J Comput Chem. 2004; 25:1656–1676. [PubMed: 15264259]
50. Oostenbrink C, Soares TA, van der Vegt NF, van Gunsteren WF. Eur Biophys J. 2005; 34:273–284. [PubMed: 15803330]
51. Berendsen, HJC.; Postma, JPM.; van Gunsteren, WF.; Hermans, J. Interaction models for water in relation to protein hydration. In: Pullman, B., editor. Intermolecular Forces. Dordrecht: D. Reidel Publishing Company; 1981. p. 331-342.
52. Oostenbrink C, Villa A, Mark AE, Gunsteren WFV. J Comp Chem. 2004; 25:1656–1676. [PubMed: 15264259]
53. Weast, RC. CRC Handbook of Chemistry and Physics 1st Student Edition. Boca Raton, Florida: CRC Pres, Inc; 1988.
54. Hess B, Bekker H, Berendsen HJC, Fraaije JGEM. J Comp Chem. 1997; 18:1463–1472.
55. Berendsen HJC, Postma JPM, DiNola A, Haak JR. J Chem Phys. 1984; 81:3684–3690.
56. Ryckaert JP, Ciccotti G, Berendsen HJC. J Comp Phys. 1977; 23:327–341.
57. Miyamoto S, Kollman PA. J Comp Chem. 1992; 13:952–962.
58. Hess B, Bekker H, Berendsen HJC, Fraaije JGEM. J Comp Chem. 1997; 18:1463–1472.
59. Kabsch W, Sander C. Biopolymers. 1983; 22:2577–2637. [PubMed: 6667333]
60. Bour P, Keiderling TA. J Phys Chem B. 2005; 109:23687–23697. [PubMed: 16375349]
61. Pancoska P, Wang L, Keiderling TA. Protein Sci. 1993; 2:411. [PubMed: 8384041]
62. Dukor RK, Pancoska P, Keiderling TA, Prestrelski SJ, Arakawa T. Arch Bioch Biophys. 1992; 298:678.
63. Lee H, Kim SS, Choi JH, Cho M. J Phys Chem B. 2005; 109:5331. [PubMed: 16863199]
64. Choi JH, Cho M. J Chem Phys. 2004; 120:4383. [PubMed: 15268607]
65. Bour P, Keiderling TA. J Chem Phys. 2003; 119:11253.
66. Ham S, Kim JH, Kochan H, Cho M. J Chem Phys. 2003; 118:3491.
67. Pantoja-Uceda D, Rico M, Jimenez MA. Biopolymers. 2005; 79:150–162. [PubMed: 16078190]
68. Buck M. Q Rev Biophys. 1998; 31:297–355. [PubMed: 10384688]
69. Grishina IB, Woody RW. Faraday discuss. 1994; 99:245–262. [PubMed: 7549540]

70. Cochran AG, Skelton NJ, Starovasnik MA. Proc Natl Acad Sci USA. 2001; 98:5578–5583. [PubMed: 11331745]
71. Susi H, Byler DM. Arch Biochem Biophys. 1987; 258:465–469. [PubMed: 3674886]
72. Shanmugam G, Polavarapu PL, Gopinath D, Jayakumar R. Biopolymers. 2005; 80:636–642. [PubMed: 15657879]

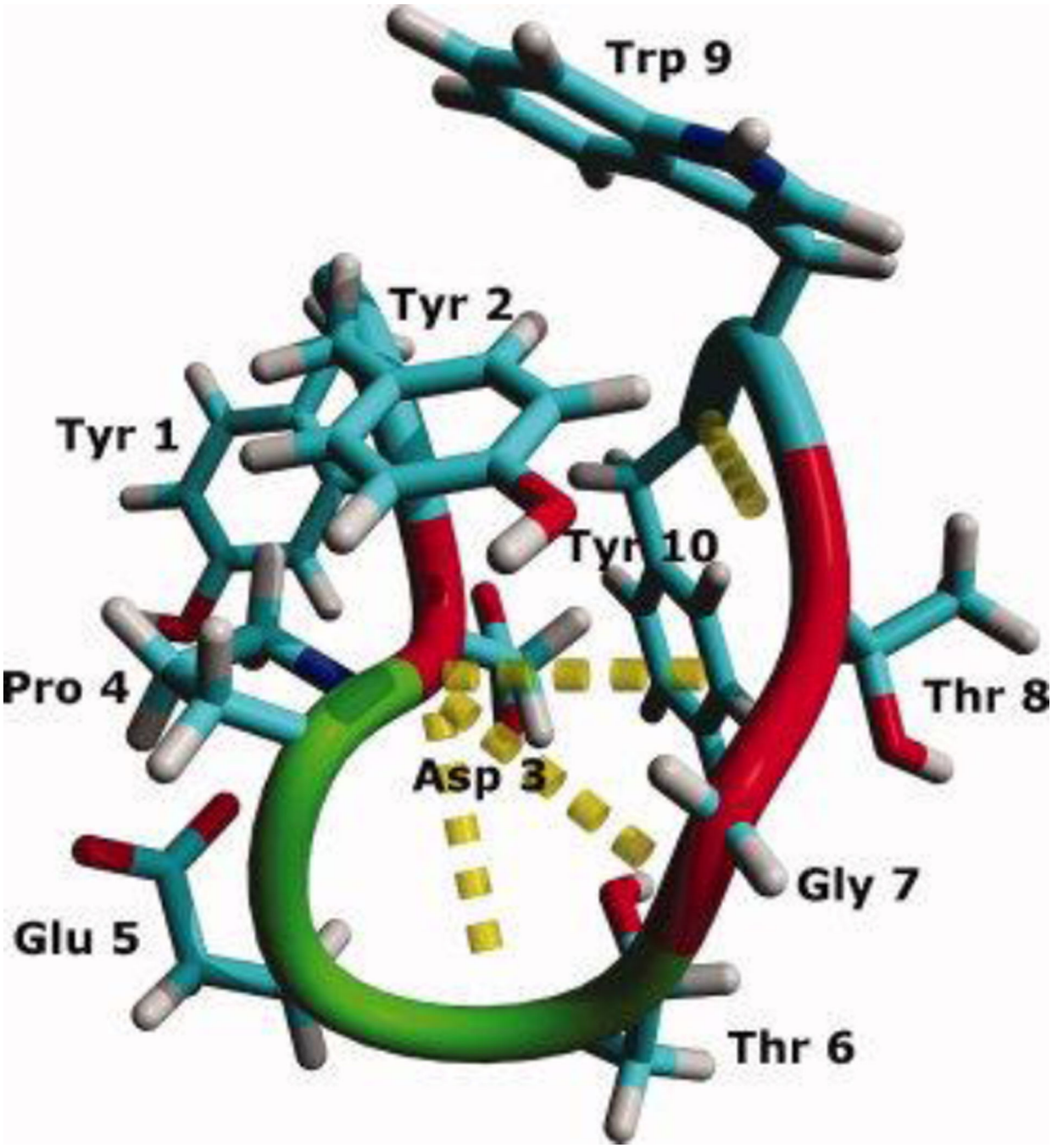

Figure 1.
The backbone and side chains of the crystal structure of CLN025. Random meander is cyan, β-sheet is red, turn is green and the H-bonds are represented by yellow dotted lines.

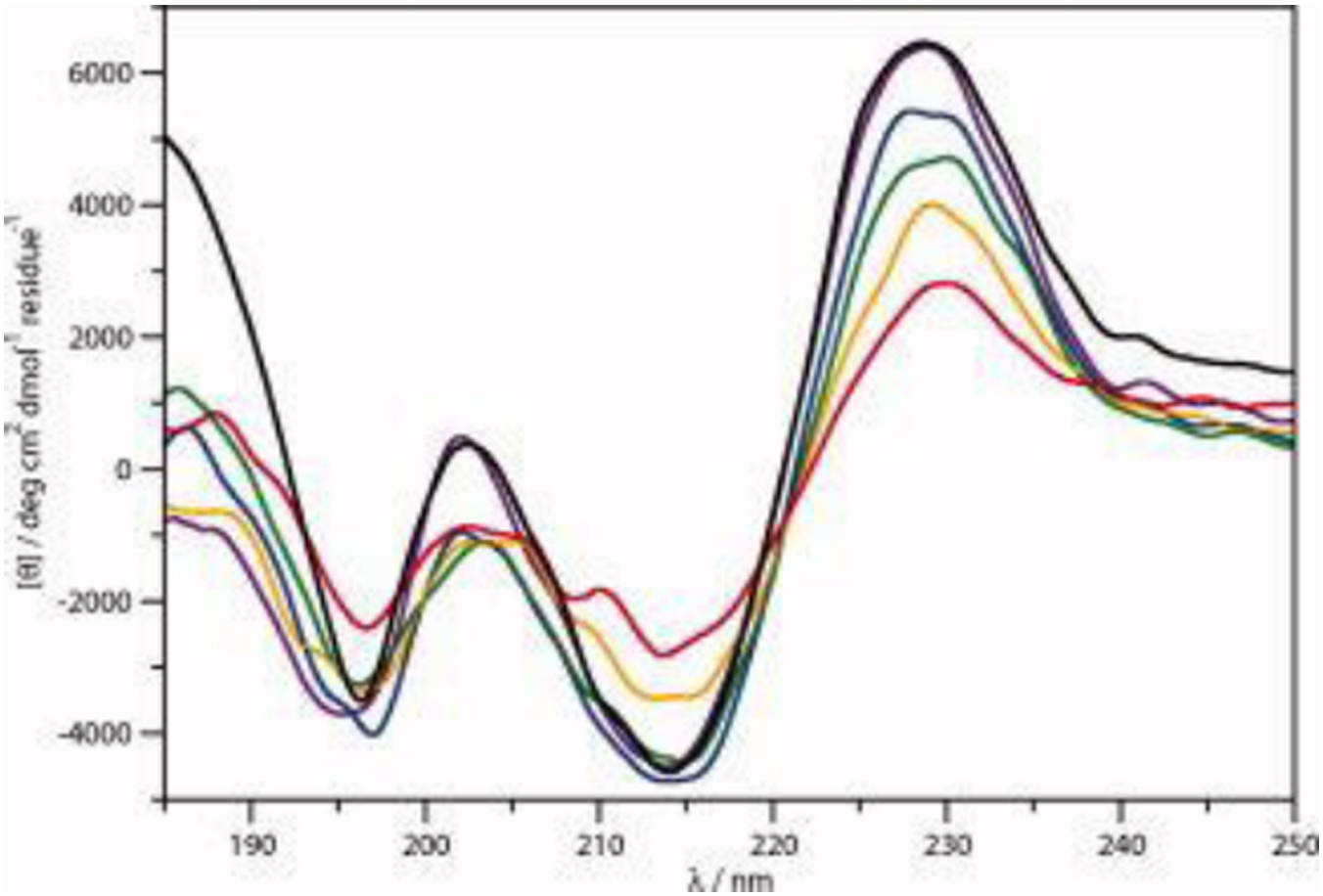

Figure 2.

The ECD spectra of 100 μM CLN025 in 20 mM potassium phosphate buffer at 0 °C (violet), 20 °C (blue), 40 °C (green), 60 °C (orange) and 80 °C (red) and cooled from 80 °C to 0 °C (black).

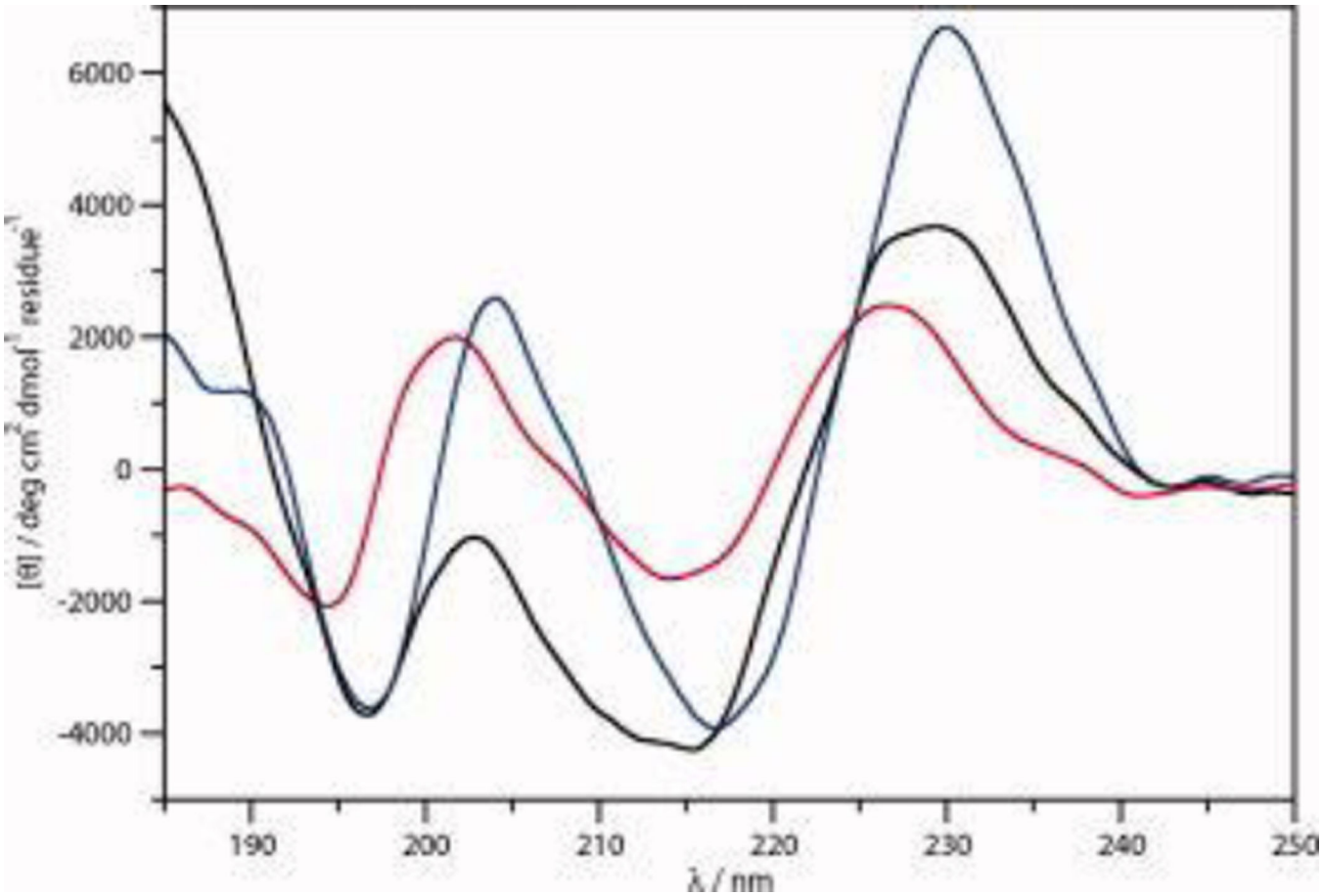

Figure 3.
The ECD spectra of 100 μM CLN025 in 20 mM potassium phosphate buffer (black), TFE (red) and MeOH (blue) at 20 °C.

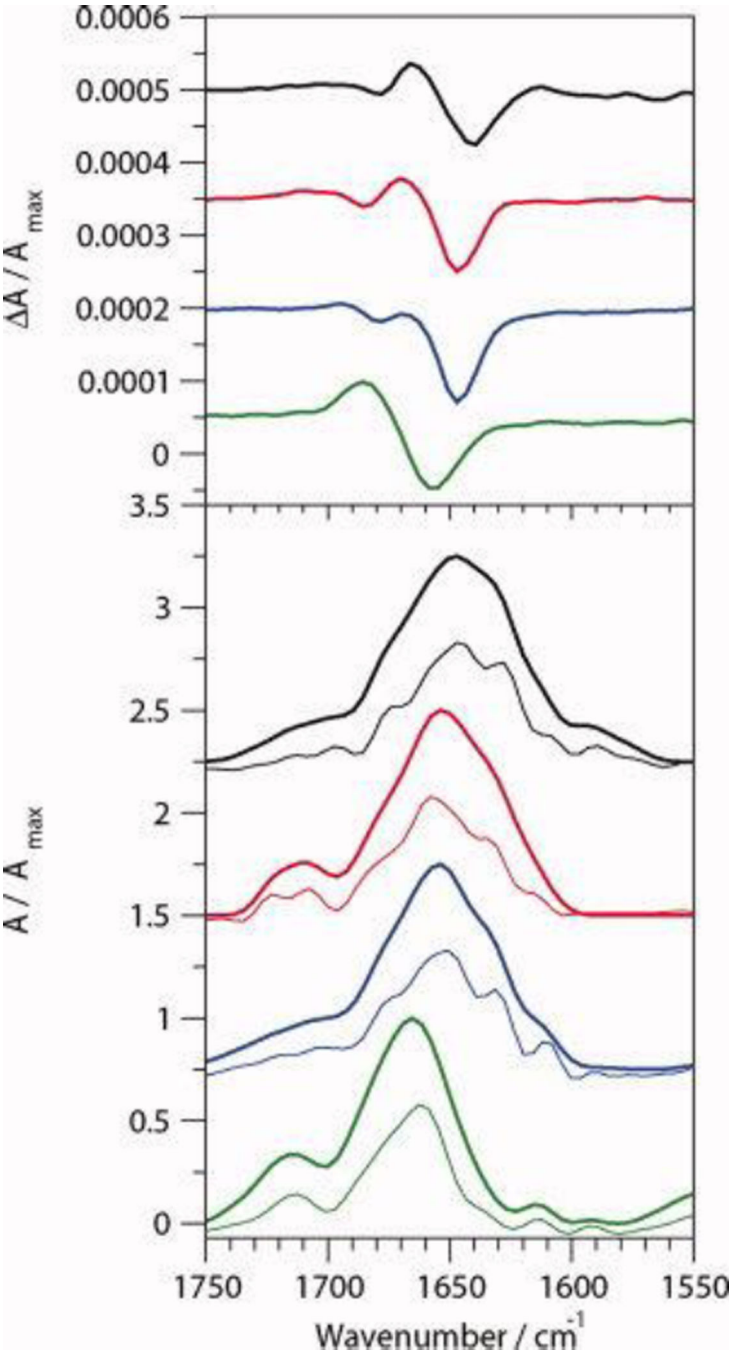

Figure 4.

Normalized VCD (top) and IR absorption (bottom) spectra of 20 mg mL^{-1} CLN025 in 5% (v/v) DMSO-d_6 in 20 mM deuterated potassium phosphate buffer (black), TFE-d (red), MeOH-d_4 (blue) and DMSO-d_6 (green). The deconvoluted absorption spectra are shown by the thin curves.

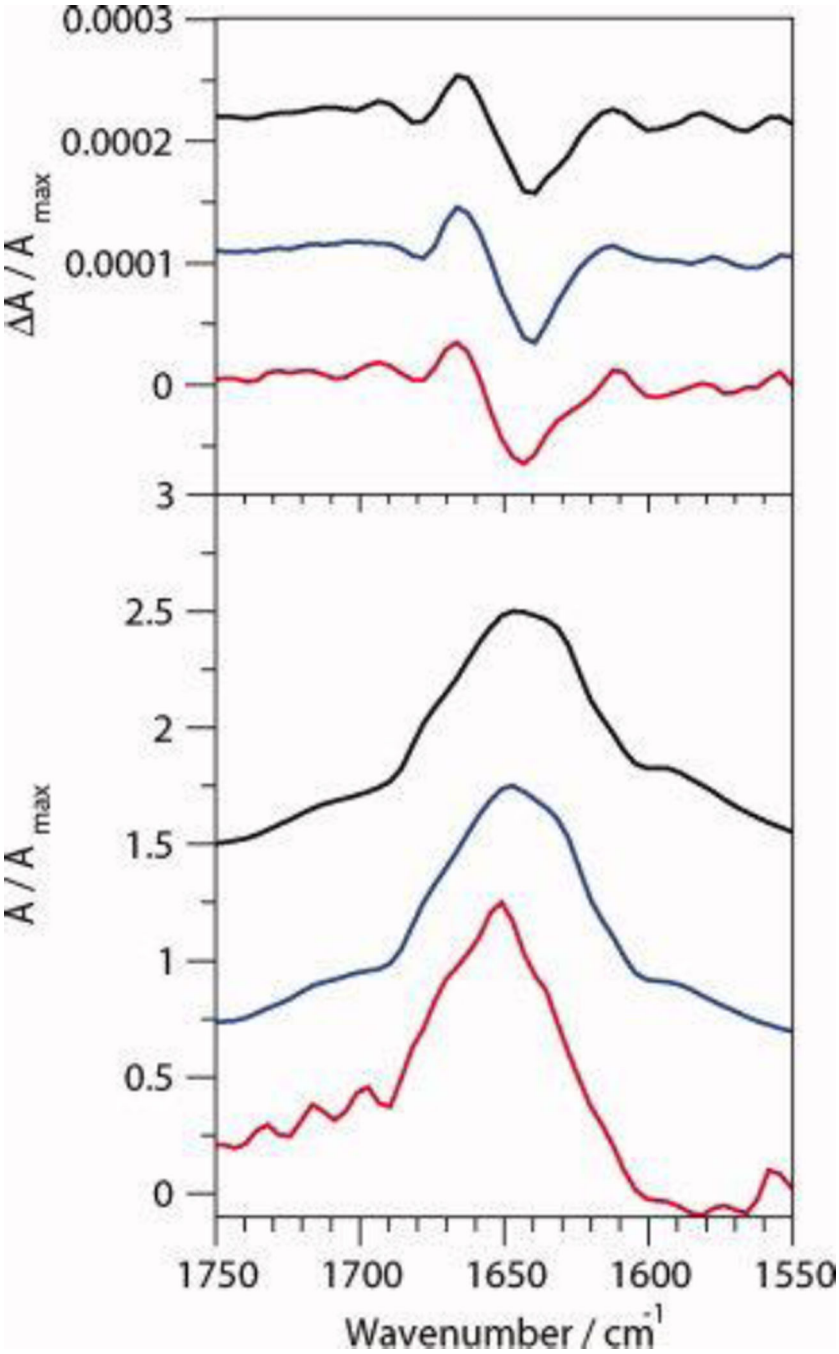

Figure 5.

Normalized VCD (top) and IR absorption (bottom) spectra of 20 mg mL^{-1} CLN025 in 5% (v/v) DMSO-d_6 in 20 mM deuterated potassium phosphate buffer at 5 °C (black), 20 °C (blue) and 60 °C (red).

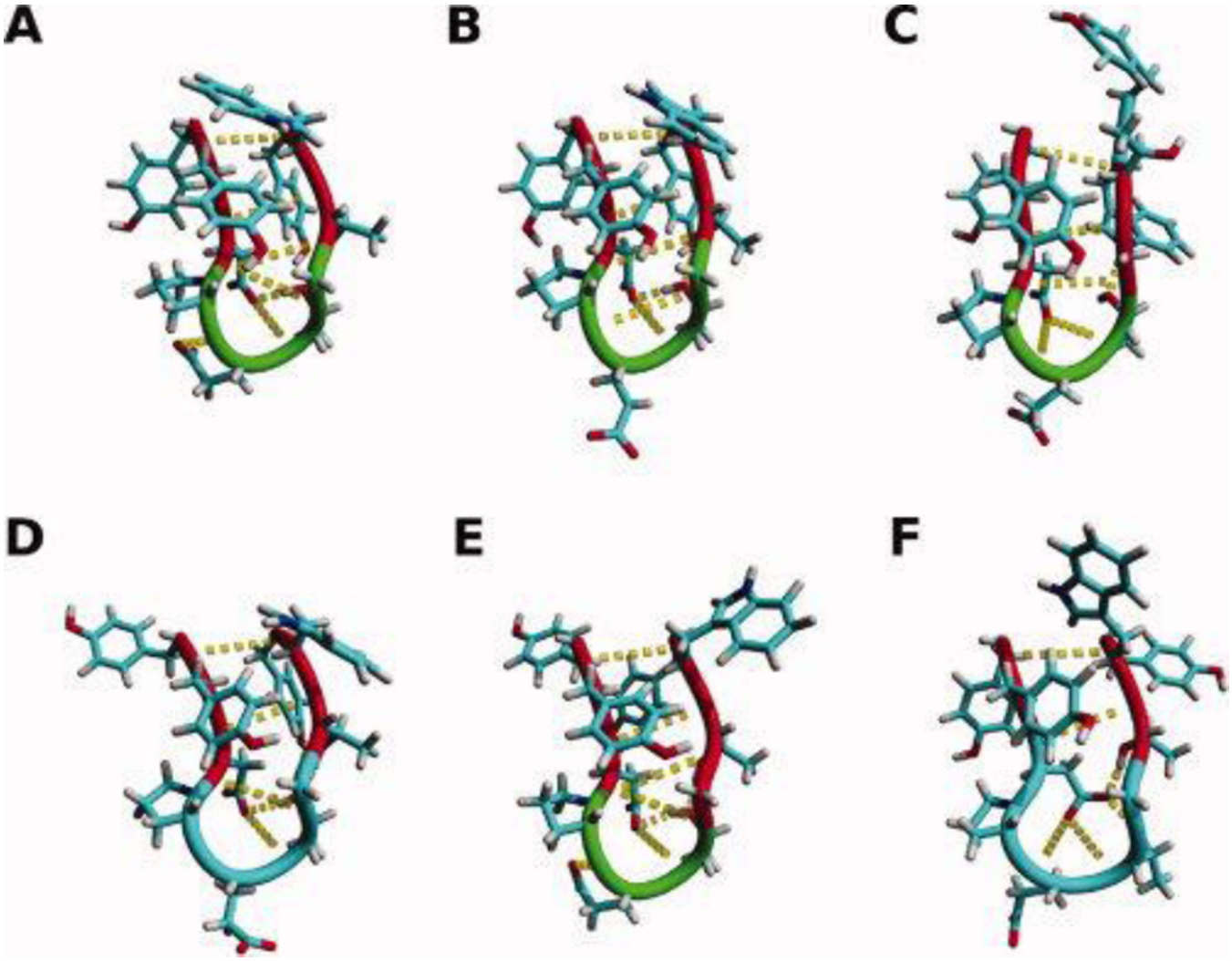

Figure 6.

The backbone and side chains of the middle structure of the most populated cluster of trajectories of MD simulations of CLN025 in **A**, H_2O 5 °C; **B**, H_2O 27 °C; **C**, H_2O 60 °C; **D**, TFE; **E**, MeOH and **F**, DMSO. Random meander is cyan, β-sheet is red, turn is green and the H-bonds are yellow dotted lines.

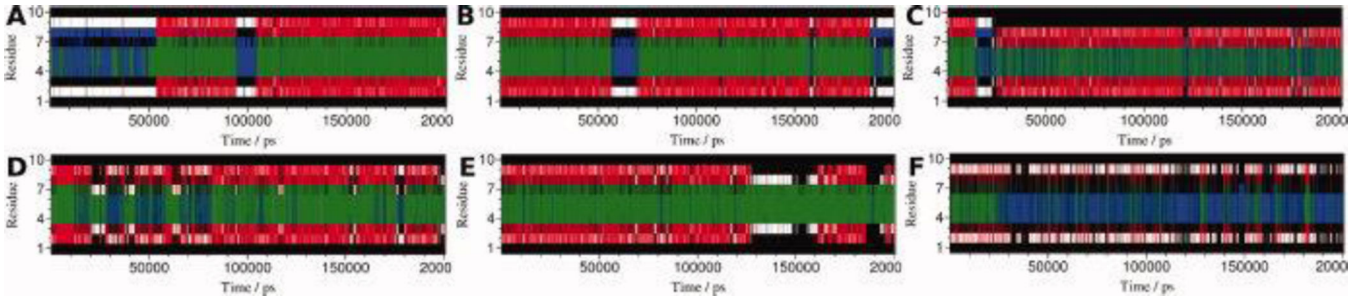

Figure 7.

DSSP analysis of the trajectories of simulations of CLN025 in **A**, H_2O 5 °C; **B**, H_2O 27 °C; **C**, H_2O 60 °C; **D**, TFE; **E**, MeOH and **F**, DMSO. Random meander is black, β-sheet is red, β-bridge is white, bend is blue and turn is green.

Table 1

Structural content (%) of CLN025 in different solvents as determined by the analysis of ECD spectra using the CDSSTR method.

Solvent*	Strand	Turn	Random meander
Buffer	46	23	31
TFE	56	24	20
MeOH	59	13	28

*See methods

Table 2

Position of bands (cm^{-1}) in the VCD spectra of CLN025

Solvent	− band	+ band	− band
Buffer	1679	1667	1640
TFE	1686	1671	1647
MeOH	1679	1671	1647
DMSO		1687	1656

Table 3

The areas of the component peaks in the deconvoluted FT-IR spectrum at the amide I' region of CLN025 as a percentage of the total area of the amide I' peak.

Wavenumber / cm^{-1}	Buffer	TFE	MeOH	DMSO	Assignment
1722		5			Turn
1712	5			24	Turn or Asp
1705		6	2		Turn or Glu
1696	2				Turn
1680		8			Turn
1675	5		5	25	Turn or β-sheet
1658	27	53	57	45	Random meander or loop
1646	40		22		Random meander
1630	16	24	11	3*	β-sheet
1612	4	4	3	3	Pro

* May be due to the low frequency absorbance of turn structure rather than β-sheet.